

Analytical Prediction of Reservoir Fluids from Rock Physics Models: A Case Study of 'X'-Field Offshore Niger Delta

Essien E. Ekom¹, Eze U. Stanley², Saleh A. Saleh³

¹ Department of Physics, University of Port Harcourt, Port Harcourt, Nigeria

² Department of Earth Science, Federal University of Petroleum Resources, Effurun, Nigeria

³ Department of Petroleum Engineering and Geoscience, Petroleum Training Institute, Effurun, Nigeria

Received August 22, 2021; Accepted December 22, 2021

Abstract

The significance of rock physics analysis in litho-fluid discrimination within a hydrocarbon reservoir using elastic rock properties can never be overstressed in reservoir characterization and hydrocarbon production. The aim of this study is to predict reservoir fluids within a hydrocarbon reservoir using elastic rock properties estimated from well log data from "X-Field" offshore Niger Delta. The reservoir intervals were identified from X-002 as HD1000 and HD2000 at depths of 5740-5780 ft and 5795-5935 ft respectively, which corresponds to the time gate 1345.00-1355.00 ms and 1355-1385 ms respectively on the seismic data. Elastic rock properties estimated within the reservoir window includes P-impedance (I_p), V_p/V_s ratio (velocity ratio), Poisson's ratio (σ), Lambda rho ($\lambda\rho$) and Mu rho ($\mu\rho$). Cross plot indicators for these properties were colour coded with density and resistivity to give a 3D picture of the attribute response. The cluster pattern on the crossplot space gives a qualitative measure of the discriminative capacity of the attributes under consideration. Cross plot of P-impedance against $\lambda\rho$ clearly delineated two zones, indicative of hydrocarbon sands and brine sands. Hydrocarbon zone (HC Sand) was identified by its low values on both Acoustic Impedance and $\lambda\rho$ axis. Theoretically, hydrocarbon sands are characterized by low density and high resistivity values, while brine sands are characterized by high density and low resistivity values. Cross plot of $\mu\rho$ versus $\lambda\rho$, showed little or no separation of the reservoir fluids on the $\mu\rho$ axis, as low value of the attribute predominates. However, there is good separation in the $\lambda\rho$ axis, making it a more fluid-sensitive attribute. Hydrocarbon zone delineated in this crossplot is suggestive of a gas filled zone based on density and resistivity values on the colour codes, as gas sand facies show lower values of $\lambda\rho$ and higher values of $\mu\rho$. All other attributes cross plots gave seemingly cluster pattern expected for hydrocarbon sands and brine sands at depths of 5758-5791 ft for brine sands, and 5904-5920 ft for hydrocarbon sands judging from the depth colour code in density versus $\lambda\rho$ cross plot. These observations are possible because each lithology responds differently to rock properties, depending on the rock fluid content and mineral properties. The results obtained shows that for detailed lithofluid prediction during hydrocarbon exploration and production, it is absolutely necessary to characterize the hydrocarbon reservoir using cross plot indicators with heightened fluid sensitivity.

Keywords: Hydrocarbon production; Elastic properties; Cross plots; Rock physics analysis; Litho-fluids discrimination.

1. Introduction

Time-lapse seismic data which is usually called "4D seismic monitoring" is a technique that is based on the analysis of repeated 3D seismic surveys. The surveys are obtained at a sizeable time interval before a field starts producing and at different post – production stages. This enables monitoring of changes in dynamic subsurface properties and fluid movement and pressure changes within the reservoir during production. This is feasible because changes in fluid saturation, pressure and other reservoir properties can give rise to differential seismic response in the subsurface reflector [1]. Assuming seismic repeatability, these changes can be transmitted to changes in the reservoir rock properties and attributes.

The amplitude recorded on a seismic trace is due to contrasts in elastic properties of rock materials at the interface separating the various layers [2]. Therefore, rock physics plays a significant role in hydrocarbon prospecting as a bridge between these elastic properties and reservoir attributes, providing the basic relationships between reservoir seismic response and lithology, pore fluid, pressure, temperature and porosity [3-4]. In general, rock elastic properties basically include compressional and shear wave velocities and density. These properties are simulated by the physical parameters of the rock, such as lithology, porosity, pore fluid and pressure [2, 5], while rock attributes refer to the combination of two or more rock properties [6].

Elastic properties being employed over time in reservoir studies include seismic velocity (compressional and shear velocities), density (ρ), P-impedance, V_p/V_s ratio, Poisson's ratio (σ), lambda-rho ($\lambda\rho$) and mu-rho ($\mu\rho$). The changes in reservoir properties caused by production can be monitored using these elastic rock properties. Rock physics analysis involves crossplotting of these elastic properties and uses rock physics models which relate rock properties to elastic properties through non-unique relationships and often in the presence of seismic data. The purpose of rock physics is for quantitative reservoir description to enable reservoir characterization by differentiating lithology and fluid [7].

Crossplotting of rock properties and attributes is one very convenient and efficient way of looking at two or more of these rock properties at the same time [8]. Most researchers in recent literature have included some form of cross-plots of seismic parameters as a way of separating hydrocarbon from the determined non-hydrocarbon background trend [7, 9-10]. Rock physics is a more sophisticated interpretation technique which shows decisively which rock properties or their attributes will be helpful to discriminate gas sands in a particular reservoir [11].

In this study, various rock properties and attributes with increased sensitivity to fluid and lithology discrimination were crossplotted to validate their fluid-sensitivity and discrimination capabilities using well log and 4D seismic data (base and monitor volumes to take advantage of 4D seismic effect) from an offshore Niger-Delta oil field, South-South Nigeria.

1.1 Geology of the study area

The study area "X-Field" lies within the Niger Delta Basin. The field is operated by Shell Petroleum Development Company (SPDC) in Nigeria. The study area "X-Field" lies within the Niger Delta Basin. The field is operated by Shell Petroleum Development Company (SPDC) in Nigeria. The study field consists of four wells as shown in the base map (Figure 1)

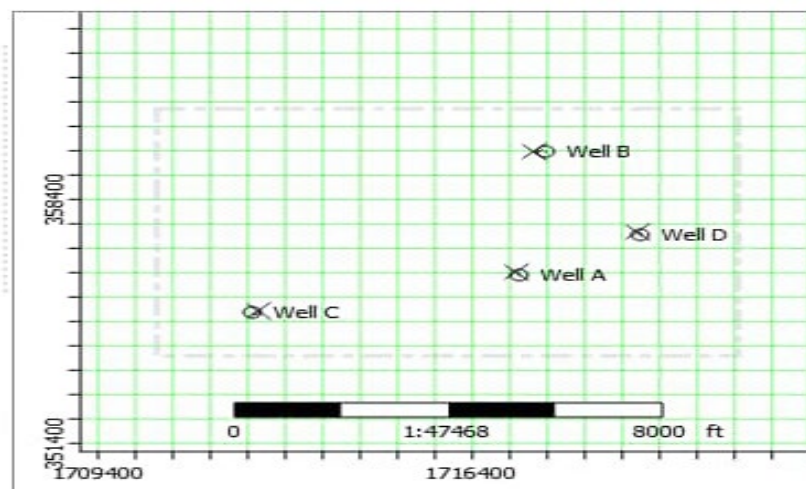


Figure 1. Base map of study area "X-Field" showing seismic lines (inlines and crosslines) for the 3D seismic acquisition, and the various well locations (Well_A, Well_B, Well_C, and Well_D)

The Niger Delta is the largest delta in Africa with a sub-aerial exposure of 75,000 km² and clastic fill of 9000–12,000 m (30,000–40,000ft) and, cease at divergent intervals by transgres-

sive sequence [12]. The Delta is a prograding depositional complex within the Cenozoic Formation of Southern Nigeria. It stretches from the Calabar flank and Abakaliki trough in Eastern Nigeria to the Benin flank in the west and opens to the Atlantic ocean in the south. It protrudes into the Gulf of Guinea as an extension from the Benue Trough and Anambra Basin provinces [13]. From the Eocene to Recent, the Delta has prograded the Southwest, forming depobelts that represents the greatest active portion of the delta at each stage of its evolution [14]. These depobelts form one of the biggest regressive deltas in the world with an area of some 300,000Km² [15], a sediment volume of 500,000km³ [16], and a sediment thickness of over 10km in the basin's depocentre [17]. The growth and augmentation of the Niger Delta commenced in Mid-Eocene by a major regression which began with the build-up of the Ameki Formation (Figure 2) west and east of the Niger river [13]. The sediment supply in the Delta is procured from two drainage systems, the Niger-Benue system through the Anambra Basin North of Onitsha (Figure 2). The stratigraphy of the Niger Delta basin is knotted by the syn-depositional sag of the clastic wedge as shale of the Akata Formation deployed under the load of prograding deltaic Agbada and fluvial Benin Formation deposits [12]. The geology, stratigraphy and structure of the region have been documented in several studies [18-23].

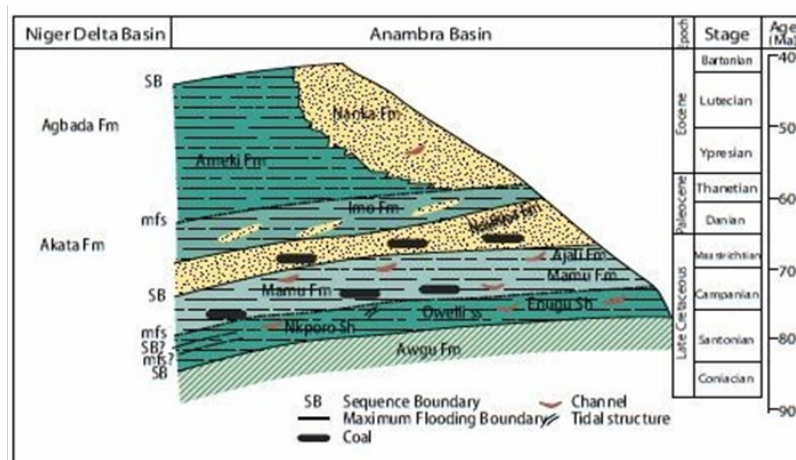


Figure 2. Stratigraphic section of the Anambra Basin from the Late Cretaceous through the Eocene and time equivalent formations in the Niger Delta. (modified from Reijer *et al.*, [24])

2. Materials and methods

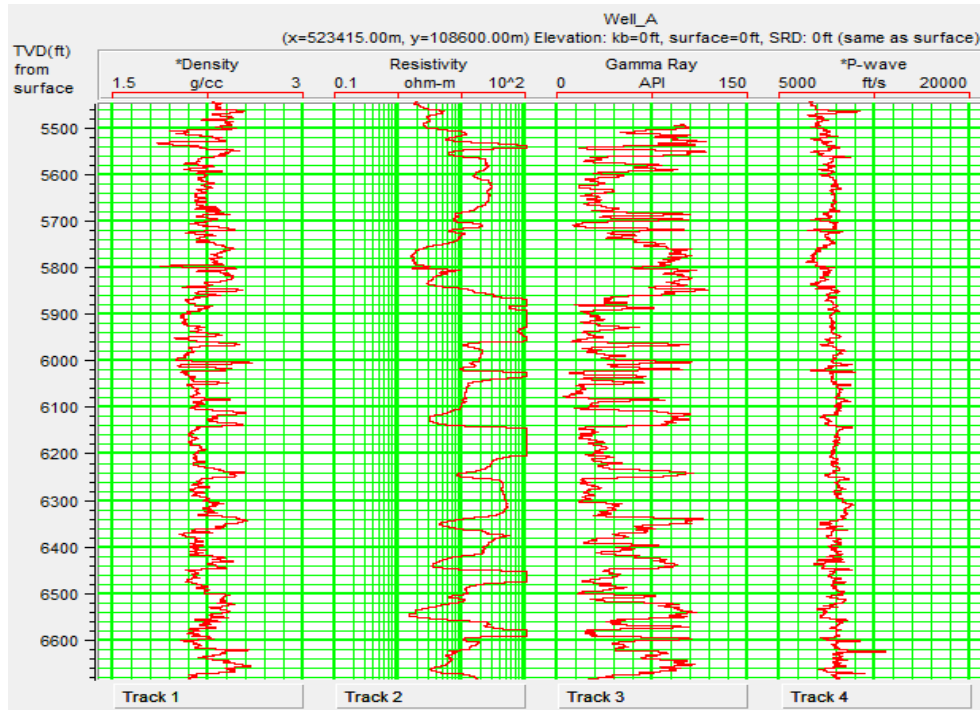
2.1. Materials

In this study, the data set used consists of suites of composite logs from three wells identified as Well_A, Well_B, and Well_C with several reservoir markers at various depths. Well_A contains Gamma ray (GR), Resistivity, Compressional sonic velocity, and Density logs to depth of 6680ft (Figure 3a). Well_B contains Gamma ray (GR), Resistivity, Compressional sonic velocity, Density, Caliper and Porosity logs to depth of 6680ft (Figure 3b), while Well_C contain Gamma ray (GR), Resistivity, Compressional sonic velocity, and Caliper logs to depth of 6500ft (Figure 3c). Also, time-lapse (4-D) seismic volume obtained from the same field in the Niger Delta was provided. The dataset was provided by Shell Petroleum Development Company (SPDC) in Port Harcourt.

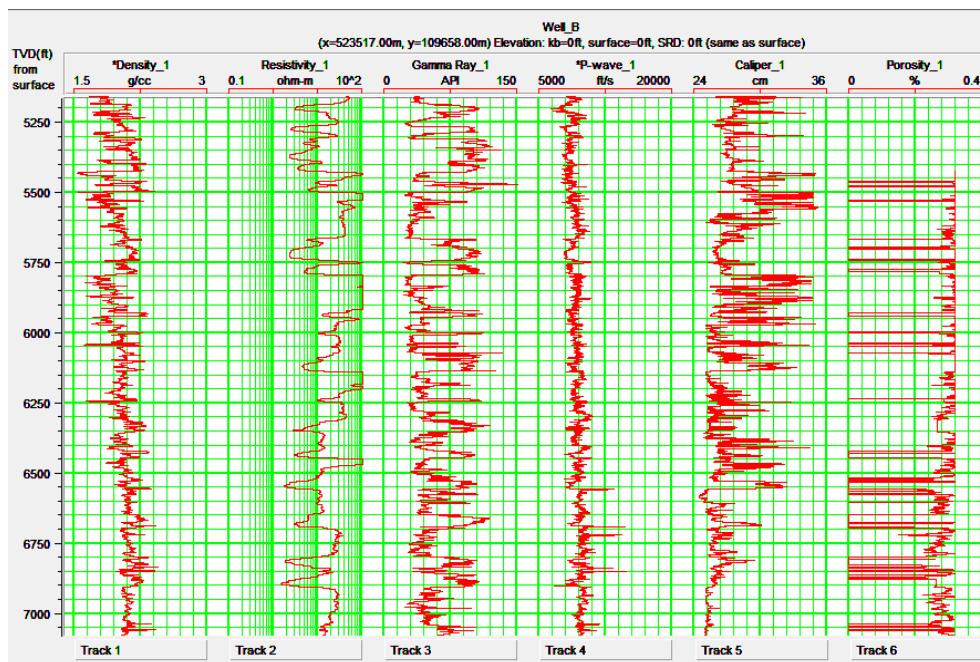
2.2. Log editing, conditioning and picking of reservoir intervals

Well logs form the basis for relating seismic properties to the reservoir. The first step in this study was to edit, normalize and interpret the well logs, before they can be used for the reservoir study [25]. This is due to occurrences like mud filtrate invasions, well-bore washouts, casing points, missing data points, and insufficient log suites during acquisition. The probable reservoir intervals were picked using a combination of low gamma ray, high resistivity, low

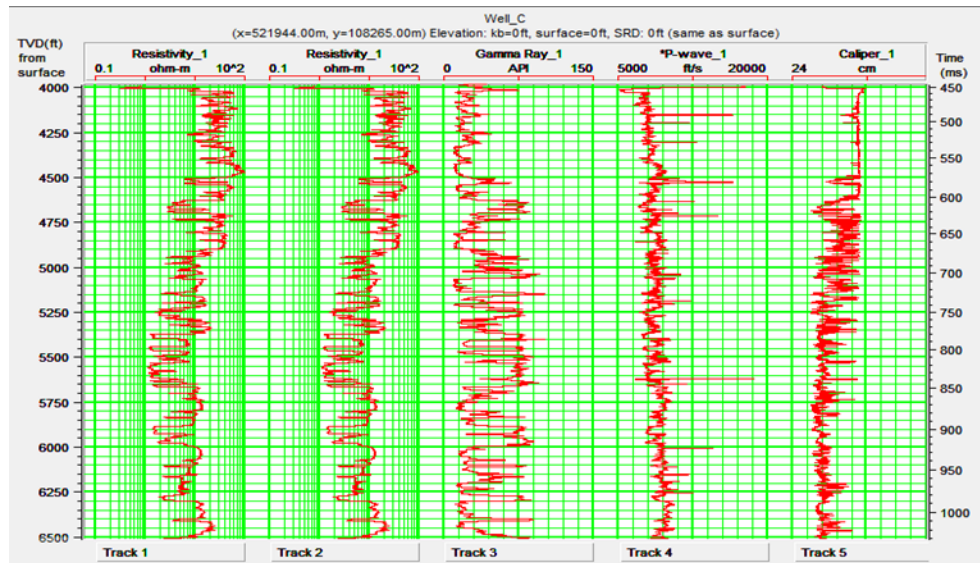
density, relatively low compressional sonic velocity, and high porosity signature within each well. The reservoir windows were marked and labelled at several depths within the depth range of the wells as reservoir markers HD1000 at depths of 5835ft-5885ft for well_A and 5740ft-5780ft for well_B, and HD2000 at depths of 5842ft-5964ft in well_A and 5795ft-5935ft in well_B (Figure, 3d). The reservoir markers HD1000 and HD2000 corresponds to the time gate 1345.00-1355.00 msec and 1355-1385 msec respectively on the base and monitor seismic sections (Figure 4a,b) when correlated using checkshot information from well_B.



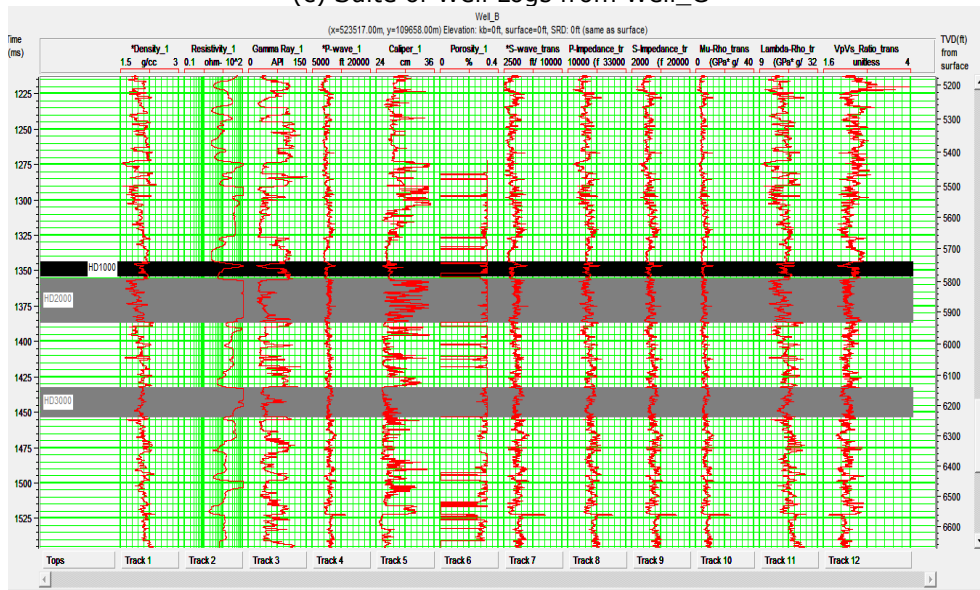
(a) Suite of Well logs from Well_A



(b) Suite of Well Logs from Well_B



(c) Suite of Well Logs from Well_C



(d) Edited and corrected logs with reservoir markers

Figure 3. (a,b,c) Suite of Well Logs from Wells_X-001, 002, 003. (d) Well log suites showing reservoir markers HD1000, and HD2000. The logs in tracks 7 – 12 were derived from the original logs using available rock physics relations. Median filter was applied to the P-wave, S-wave and density logs to remove the high frequency components effect

2.3. Rock property and attribute crossplots

In this study, from the original well logs provided, S-wave sonic log (V_s) was empirically generated from the corrected P-wave sonic log using Castagna *et al.*,^[26] V_p - V_s relation for sedimentary basins given as:

$$V_p = 1.16 V_s + 1360 \text{ (in m/sec)} \quad (1)$$

where; V_p = compressional wave velocity; V_s = Castagna derived shear wave velocity; 1.16 and 1360 are constants.

Next was the estimation of elastic rock properties such as P-impedance, Velocity (V_p - V_s ratio), poisson's ratio and Lamé parameters. These properties were estimated from the logs using Goodway *et al.*,^[27] relation, and the calculated P-wave and S-wave velocities.

This relations are given as:

$$P\text{-imp} = V_p * \rho \quad (2)$$

$$\text{Velocity ratio (} V_p/V_s \text{ ratio)} = V_p/V_s \quad (3)$$

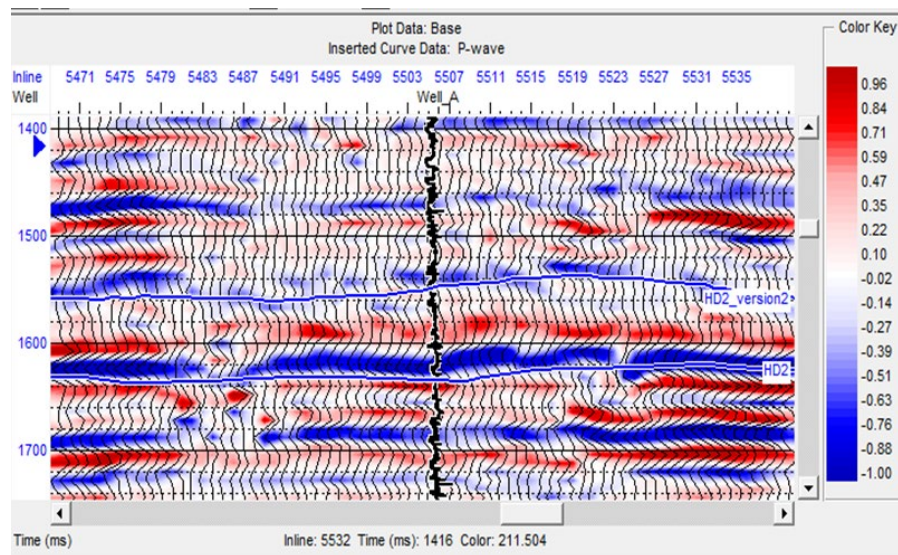
$$\text{Incompressibility (} \lambda \rho \text{)} \lambda \rho = (\rho V_p)^2 - 2(\rho V_s)^2 \quad (4)$$

$$\text{Rigidity modulus (} \mu \rho \text{)} \mu \rho = (\rho V_s)^2 \quad (5)$$

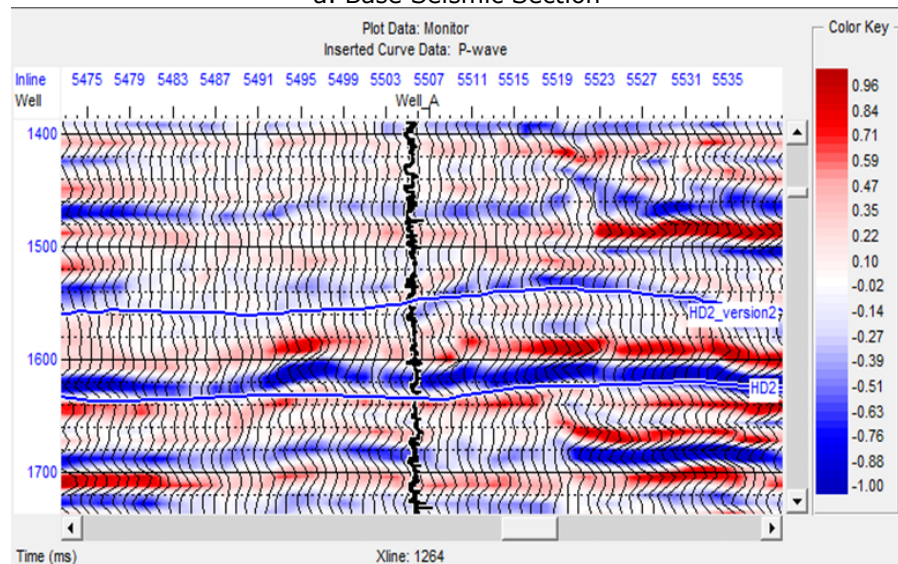
$$\text{Poisson's ratio (} \phi \text{)} = \lambda/2 (\lambda + \mu) \quad (6)$$

where: P-imp (Ip) = compressional wave acoustic impedance (the product of P-velocity and density); V_p/V_s ratio = ratio of P-velocity to S-velocity; ρ = rock density.

These properties can be used in lithology and fluid discrimination within a reservoir formation [28-29]. $\lambda \rho$ and $\mu \rho$ are called Lamé parameters. $\lambda \rho$ (Lamda rho) is called incompressibility and is sensitive to pore fluids while $\mu \rho$ (Mu rho) called rigidity is sensitive to rock frame matrix. The Lamé parameters $\lambda \rho$ and $\mu \rho$ crossplots were used to discriminate litho-fluids and lithofacies within the reservoir. Crossplots of these rock properties were plotted using Hampson Russell software to investigate their fluid discriminative capability. The colour code gives a 3D view of the attributes' responses, and the pattern of clusters on the crossplot space gives a quantitative measure of discrimination.



a. Base Seismic Section



b. Monitor Seismic Section

Figure 4. (a, b) Base and Monitor Seismic Volumes with inserted P-wave logs (from Well_A) and Seismic Horizons (HD2 and HD_Version2).

3. Results and discussion

Crossplots of rock attributes are shown in Figures 5-9. In each crossplot, two zones, indicative of Hydrocarbon sands (red ellipse) and Brine sands (blue ellipse) were identified and marked. This deduction was based on the expected characteristics responses of fluids to the attributes under consideration. Figure 5(a, b) shows the crossplot of P-wave acoustic impedance (P-impedance) against Lambda-rho (incompressibility), colour coded with density and resistivity logs. Hydrocarbon filled sands (Figure 5a) and Brine filled sands (Figure 5b) are identified from the pattern of clusters. The hydrocarbon zone (HC Sand) is recognized by its low attribute values on both the acoustic impedance and Lambda-rho axis as expected. The hydrocarbon sands are characterized by low values of density and high values of resistivity, while the brine sands are marked by high density and low resistivity values as theoretically expected [29-30]. In Mu-rho (rigidity) on the vertical-axis versus Lambda-rho (incompressibility) on the horizontal-axis crossplot, colour coded with density and resistivity (Figure 6a,b), there is little or no separation of reservoir fluids on the Mu-rho axis. Gas sand facies show lower values of Lambda-rho and higher values of Mu-rho [29]. Low values of the attributes predominates, as clusters are predominantly at the base of the Mu-rho axis. There is, however, good separation in the Lambda-rho (horizontal) axis, making it a more fluid-sensitive attribute. Therefore, hydrocarbon zone delineated in this crossplot is suggestive of a gas filled zone judging from density and resistivity colour codes (Figure 6a,b), which clearly separates the hydrocarbon zone from the brine zones. Poisson's ratio (vertical axis) versus Lambda-rho (horizontal axis) crossplot is shown Figure 7(a,b). Poisson's ratio is a good litho-fluid indicator [9, 29] and high Poisson's ratio (≈ 0.5) is indicative of gas sand lithofacies. However, the range of Poisson's ratio observed in the crossplot is between 0.325 and 0.425 (Figure 7). Fluids are not clearly discriminated within the axis, as the values of the attribute overlap for hydrocarbon and brine sand zones. The fluids are better defined in the Lambda-rho axis. The colour distribution for the zones (Resistivity and Density) agree with theoretical values. Crossplot of acoustic impedance (I_p) versus V_p/V_s ratio is shown in Figure 8. High values of V_p/V_s ratio ($V_p/V_s > 2$) is indicative of Shale lithofacies [26]. However, the attributes are not very discriminative of fluid types as observed in the pattern of clusters shown in Density (Figure 8a) and Resistivity (Figure 8b) colour codes. Crossplot of density versus Lambda-rho (incompressibility) colour coded with depth (Figure 9a) and resistivity (Figure 9b), shows fairly good discrimination of fluids.

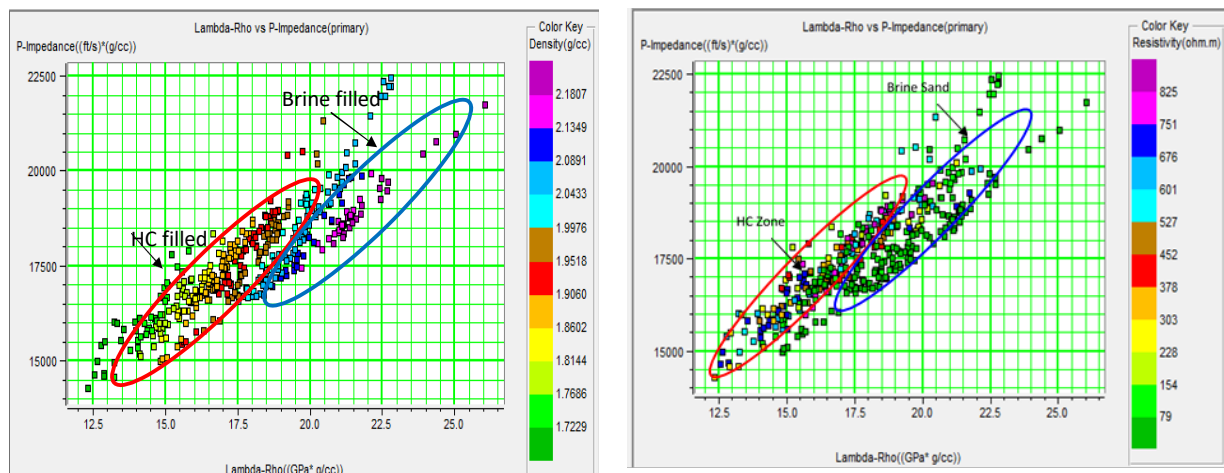


Figure 5. Crossplot of P-Impedance against Lambda-rho (λ) colour-coded with (a) density (b) resistivity

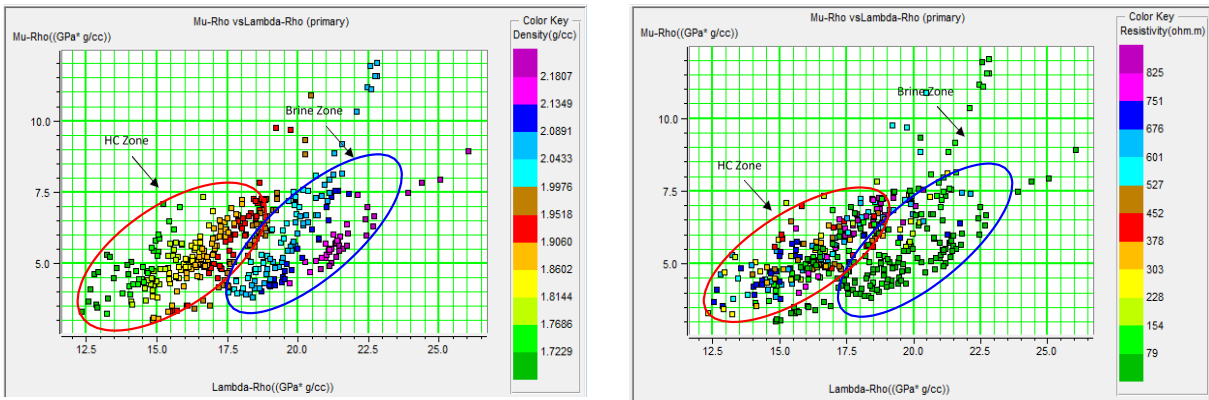


Figure 6. Mu-rho (μ) versus lambda-rho (λ) crossplot, colour-coded with (a) density (b) resistivity
Clusters pattern show discrimination between hydrocarbon (HC) and Brine zones.

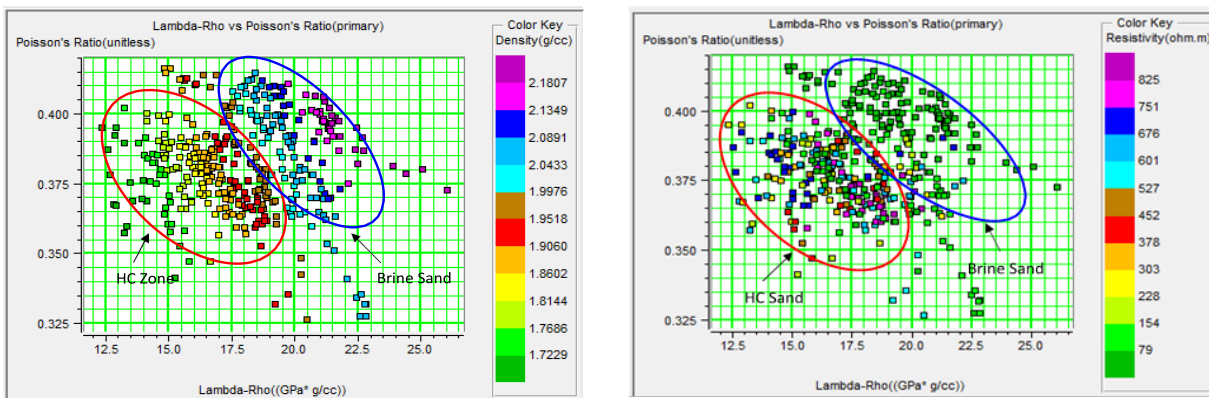


Figure 7. Poisson's Ratio (σ) versus Lambda-Rho (λ) crossplot colour-coded with (a) Density (b) Resistivity. Crossplots show two regions of clusters identified as hydrocarbon filled sand and brine filled sands

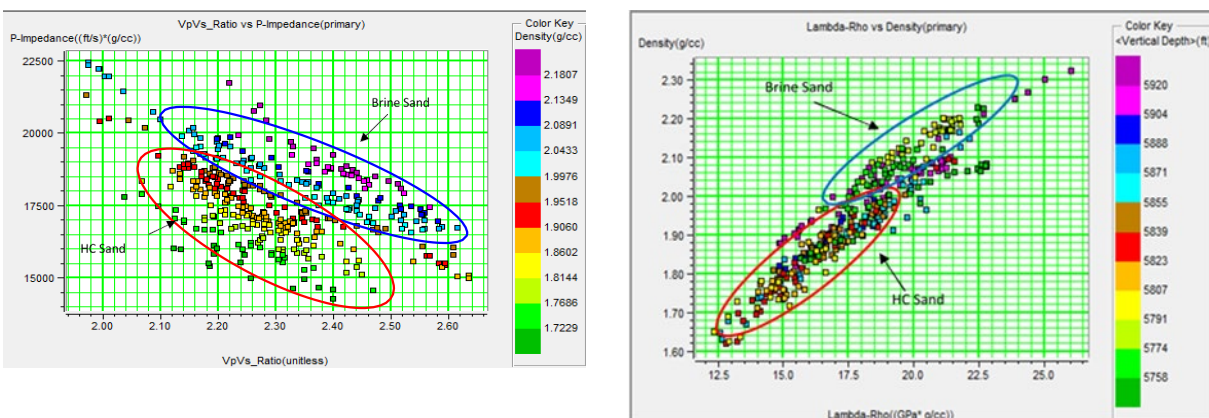


Figure 8. Impedance versus Vp/Vs Ratio Crossplot (a) colour-coded with density (b) colour-coded with resistivity

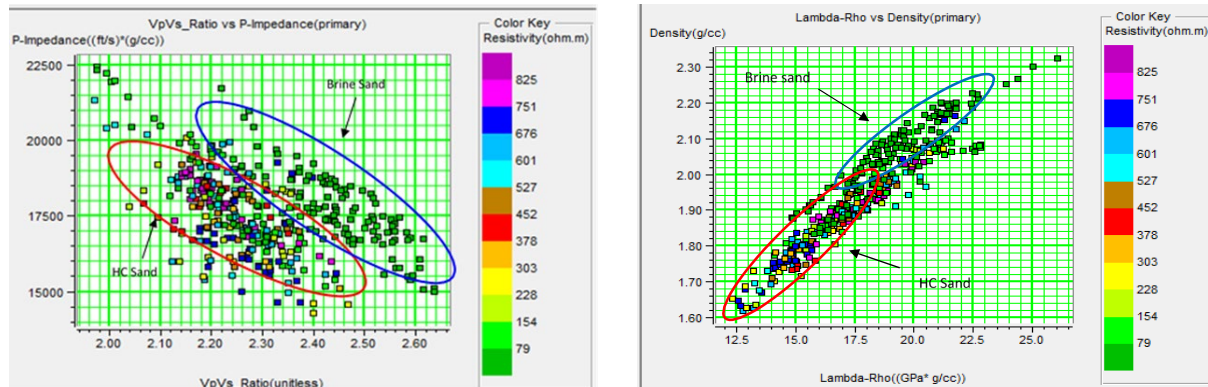


Figure 9. Crossplot of Density against Lambda-rho colour-coded with (a) Vertical Depth (b) Resistivity. The fluids are fairly discriminated. There is, however, some overlap in the colour codes.

4. Conclusion

The application of rock physics analysis in lithofacies and litho-fluid discrimination within a hydrocarbon reservoir using elastic rock properties can never be over emphasized for detailed reservoir imaging in hydrocarbon exploration and production. Elastic rock properties estimated within the reservoir window includes P-impedance (I_p), Vp/Vs ratio (velocity ratio), Poisson's ratio (σ), λ_p (incompressibility), and μ_p (rigidity). Cross plot indicators for these properties were colour coded with density and resistivity to give a 3D picture of the attribute's response. The cluster pattern on the crossplot space gives a quantitative measure of the discriminative capacity of the attributes under consideration. The cross plot of P-impedance against Lambda-rho clearly demarcated two zones, indicative of Hydrocarbon sands and Brine sands based on the expected characteristics responses of the attributes. The hydrocarbon zone (HC Sand) was recognised by its low values on both the Acoustic Impedance and Lambda-rho axis, since hydrocarbon sands are characterized by low values of density and high values of resistivity, while brine sands are marked by high density and low resistivity values. Crossplot of μ_p versus λ_p , showed little or no separation of reservoir fluids on the μ -rho axis, as low values of the attributes predominates, however, there is good separation in the λ_p axis, making it a more fluid-sensitive attribute. The hydrocarbon zone delineated in this crossplot is suggestive of a gas filled zone based on density and resistivity values on the colour codes, as gas sand facies show lower values of λ_p and higher values of μ_p . All other attributes crossplots gave seemingly cluster pattern expected for hydrocarbon sands and brine sands within depth 5758-5791 ft for brine sands, and 5904-5920 ft for hydrocarbon sands judging from the depth colour code in density versus λ_p crossplot. These observations are possible because each lithology has a different rock property response that is subject to litho-fluid and mineral property content. The result obtained shows that for comprehensive litho-fluid prediction during hydrocarbon exploration and production, it is imperative to characterize the hydrocarbon reservoir in terms of its litho-fluid content and lithology using cross-plot indicators with enhanced susceptibility to fluid and lithology discrimination.

Acknowledgement

We wish to express our gratitude to Shell Petroleum Development Company (SPDC) Port Harcourt for providing the data used for this study, and also to CGG Geosoft for providing the software used for the study.

Funding

There was no grant or financial support provided from any agency in the public, commercial and not-for profit organization for this research work

Conflicts of interest/Competing interests

We declare that this research work has never been submitted previously by anyone to any journal for peer review and publication; hence it is an original work. All the ethical principles of research in the data collection, preparation, analysis and interpretation were implemented.

Availability of data and material

Not applicable.

Code availability (Software used)

Hampson Russell software program.

References

- [1] Landro M. Discrimination Between Pressure and Fluid Saturation Changes from Time – Lapse Seismic Data. *Geophysics*, 2001; 66: 836-844.
- [2] Ogagarue DO, Anine LA. An Integration Of Rock Physics, AVO Modeling and Analysis For Reservoir Fluid And Lithology Discrimination in a Niger Delta Deep water block. *Journal of Applied Geology and Geophysics*, 2016; 4(2): 36-46.
- [3] Chi XG, Han DH. Lithology and Fluid Differentiation Using a Rock Physics Template. *The Leading Edge*, 2009; 28: 60-65.
- [4] Munyithya JM, Ehirim CN, and Dagogo T. Rock Physics Models and Seismic Inversion in Reservoir Characterization, "MUN" Onshore Niger Delta Field. *International Journal of Geosciences*, 2019, 10: 981-994.
- [5] Tathan RH. Vp/Vs and lithology, *Geophysics*, 1982; 47: 336-344.
- [6] Sherrif RE, Geldart LP. *Exploration Seismology*. 2nd ed. Cambridge University Press, New York, 1995: 54-56.
- [7] Abe SJ, Olowokere MT, Enikanselu PA. Development of Model for Predicting Elastic Parameters in 'Bright' Field, Niger Delta Using Rock Physics Analysis. *NRIAG Journal of Astronomy and Geophysics*, 2018; 7: 264-278.
- [8] Burianyk, M. Amplitude-vs- Offset and Seismic Rock Property Analysis: A Primer. *The Canadian Society of Exploration Geophysicist Recorder*, 2000; 11: 1-14.
- [9] Nnorom SL, Eze S, Saleh AS, Wilson EO. Application of Rock physics modelling for lithofluids discrimination within a hydrocarbon reservoir interval: A case study of 'X'-Field offshore Niger Delta. *Petroleum Technology Development Journal*, 2020; 10(2): 56-72.
- [10] Omudu LM, Ebeniro J O, Osayande N, Adesanya, S. Lithology and fluid discrimination from elastic rock properties cross-plot: Case study from Niger Delta. *Proceeding, 24th Annual International Conference and Exhibition of Petroleum Explorationist (NAPE) 2006*.
- [11] Dewar J. Rock Physics For The Rest of Us- An Informal Discussion. *The Canadian Society of Exploration Geophysicists Recorder*. 2001; 5: 43-49.
- [12] Short KC, Stauble AJ. Outline of geology of Niger Delta. *AAPG Bulletin*. 1967, 51(5): 761-779.
- [13] Etu-Efeotor JO. *Fundamentals of Petroleum Geology*. Paragraphics, Port Harcourt. 1997: 84-87.
- [14] Doust H, Omatsola E. Niger Delta. In Edwards JD & Santogoss, PA. (Eds.), *Divergent and Passive Marine Basins*. American Association of Petroleum Geologists, Memoir, 1990; 48: 239 -248.
- [15] Kulke H. *Regional Petroleum Geology of the World. Part II: Africa, America, Australia and Antarctica*: Berlin, Gebrüder Borntraeger, 1995: 43- 172.
- [16] Hospers J. Gravity field and structure of the Niger Delta, Nigeria, West Africa: *Geological Society of American Bulletin*. 1965; 76: 407-422.
- [17] Kaplan A, Lusser CU, Norton IO. Tectonic map of the world, panel 10: Tulsa, American Association of Petroleum Geologists, scale 1:10,000,000, 1994.
- [18] Weber KJ, Daukoru EM. *Petroleum Geology of the Niger Delta Proceedings of the 9th World Petroleum Congress Tokyo*. Appl. Sci. publishers, Ltd, London, 1975;2: 202-221.
- [19] Avbovbo AA. Tertiary lithostratigraphy of Niger Delta, *Am. Assoc. Pet. Geol. Bull.* 1978; 62: 295-300.
- [20] Evamy BD, Haremboure J, Kammerling R, Knaap WA, Molloy FA, Rowlands PH. Hydrocarbon habitat of tertiary Niger Delta. *AAPG Bulletin*. 1978; 62(1): 1 - 39.
- [21] Whiteman AJ. *Nigeria: its petroleum Geology resources and potential 1 and 2*. Graham and Trotter, London, 1892: 394.
- [22] Owoyemi AO, Wills A. Depositional patterns across syndepositional normal faults Niger Delta Nigeria. *J Sediment Res.* 2006; 76:346-363.

- [23] Bilotti F, Shaw JH. Deepwater Niger Delta Fold and Thrust Belt modeled as a Critical – Taper Wedge: The Influence of Elevated Basal Fluid Pressure on Structural Styles. AAPG Bulletin. 2005; 89(11): 1475-1491.
- [24] Reijers TJA, Petter S W, Nwajide CS. The Niger Delta Basin: In Reijers TJA., ed.,: Selected Chapter on Geology: SPDC, Warri. 1997: 103-118.
- [25] Carr M, Cooper R, Smith M, Turham T, Taylor G. Generation of Rock and Fluid Properties Volume via The Integration of Multiple Seismic Attributes and Log data. EAGE. First Break. 2001; 19: 567-574.
- [26] Castagna JP, Bazle ML, Eastwood RL. Relationships Between Compressional Wave and Shear Wave Velocities in Clastic Silicates. Geophysics. 1985; 50(4): 571 – 581.

To whom correspondence should be addressed: Eze U. Stanley, Department of Earth Science, Federal University of Petroleum Resources, Efurun, Nigeria, E-mail: uchechukwueze2014@gmail.com